THE ASTROPHYSICAL JOURNAL, 341:839–846, 1989 June 15

OBSERVATIONS OF VARIOUS METHANOL MASER TRANSITIONS TOWARD THE NGC 6334 REGION

KARL M. MENTEN
Harvard-Smithsonian Center for Astrophysics
AND
WOLFGANG BATRLA
National Radio Astronomy Observatory
Received 1988 September 6; accepted 1988 December 1

ABSTRACT

We have used the Green Bank 140 foot telescope to observe a number of CH_3OH lines toward the H II region F in the NGC 6334 star-forming region. We discovered strong maser emission in the $2_1 \rightarrow 3_0 E$ and $9_2 \rightarrow 10_1 A^+$ transitions at 19.9 and 23.1 GHz, respectively. These masers have velocities that are identical to the velocities covered by some components of the strong maser emission observed in the 12.1 GHz $2_0 \rightarrow 3_{-1} E$ line.

We detected thermal emission in the 25 GHz $J_2 \rightarrow J_1 E$ line toward the molecular core associated with NGC 6334-F and toward a cool dust continuum source to the north of the H II region. Toward the northern source we also detected maser emission from the $J_2 \rightarrow J_1 E$ lines. From these observations and a comparison with published data on W3(OH), we suggest that while the 12.1, 19.9, and 23.1 GHz methanol masers appear closely associated with compact H II regions and OH masers, the 25 GHz masers may be associated with dense condensations in an earlier evolutionary state.

Subject headings: interstellar: molecules — masers — nebulae: H II regions — nebulae: individual (NGC 6334)

I. INTRODUCTION

Maser emission from interstellar methanol (CH_3OH) was first observed in the 25 GHz $J_{k=2} \rightarrow J_{k=1} E$ ($J = 4, 5, 6, \ldots$) transitions of the molecule's E symmetry species toward the Orion-KL region (Barrett, Schwartz, and Waters 1971); more of these "Orion-type" masers have been found in a number of sources (Menten *et al.* 1986*a*). Wilson *et al.* (1984, 1985) have discovered another class of methanol maser emission in the $9_2 \rightarrow 10_1 A^+$ and $2_1 \rightarrow 3_0 E$ lines, at 23.1 and 19.9 GHz, respectively, toward the H II region W3(OH). Several facts indicate that the W3(OH) methanol masers are of a different nature than the Orion-type masers (observed in the $J_2 \rightarrow J_1 E$ lines): (*a*) none of the $J_2 \rightarrow J_1 E$ masers shows maser action in the $9_2 \rightarrow 10_1 A^+$ and $2_1 \rightarrow 3_0 E$ lines; (*b*) the $J_2 \rightarrow J_1 E$ lines are seen in absorption toward W3(OH); (*c*) VLA studies of the $9_2 \rightarrow 10_1 A^+$ transition toward W3(OH) (Menten *et al.* 1988*a*) show that in this source the maser emission arises from several condensations which appear projected on the ultracompact H II region in the same areas as the OH masers, whereas $J_2 \rightarrow J_1 E$ masers are mostly found offset from compact continuum and infrared sources and other molecular maser centers (Menten *et al.* 1986*a*).

Subsequently, very strong maser emission in the $2_0 \rightarrow 3_{-1} E$ line at 12.1 GHz was detected toward W3(OH), the compact continuum source F (Rodríguez, Cantó, and Moran 1982) in NGC 6334, and many other sources (Batrla *et al.* 1987; Norris *et al.* 1987; Koo *et al.* 1988). Recently, a VLBI experiment has shown that in the case of W3(OH) the 12.1 GHz masers are located in the same region as the 23.1 GHz masers, implying that both maser transitions need similar conditions for their excitation (Menten *et al.* 1988*b*). Nevertheless, it is clear that 12.1 GHz maser emission is a much more widespread phenomenon than 19.9 or 23.1 GHz masers, since Wilson *et al.* (1984, 1985) and Menten (unpublished data) did not find additional masers in the latter two lines, although their samples included a number of 12.1 GHz maser sources. If W3 (OH) represents a distinct class of methanol maser, then others in this class may be recognized from more complete surveys of the $9_2 \rightarrow 10_1 A^+$ and $2_1 \rightarrow 3_0 E$ lines. A promising candidate is NGC 6334-F[1] which resembles W3(OH) in that (*a*) it shows very strong 12.1 GHz emission; (*b*) OH masers are associated with the compact continuum source (Gaume and Mutel 1987; Zheng *et al.* 1988); and (*c*) methanol and OH maser emission cover the same velocity range (see Fig. 2 of Batrla *et al.* 1987). To investigate further the similarities between W3(OH) and NGC 6334-F, we have observed toward NGC 6334-F a number of K band methanol lines with frequencies between 19.9 and 25.3 GHz including all transitions that are known to show maser action toward W3(OH).

II. OBSERVATIONS

The observations were made between 1987 April 7 and 10 with the 140 foot telescope of the NRAO[2] in Green Bank. Two K band maser receivers were used simultaneously utilizing the newly installed beam splitter to detect orthogonal linear polarizations. With this receiver setup and the autocorrelator split in four parts of 256 channels each, usually two lines were observed at the same time. For most of the observations, two of the autocorrelator modules were used with bandwidths of 5

[1] Unfortunately, the nomenclature of objects in the NGC 6334 region is very confusing. The position of the continuum source F coincides with the OH maser source NGC 6334 A, also known as NGC 6334 N. The associated near-infrared source has been labeled IRS 1, while in the far-infrared literature most frequently the designation NGC 6334-I is used. A cool dust continuum source is situated $\approx 2'$ north of NGC 6334-F and is sometimes called NGC 6334-I(North), the designation we will use.

[2] The National Radio Astronomy Observatory is operated by Associated Universities, Inc., under cooperative agreement with the National Science Foundation.

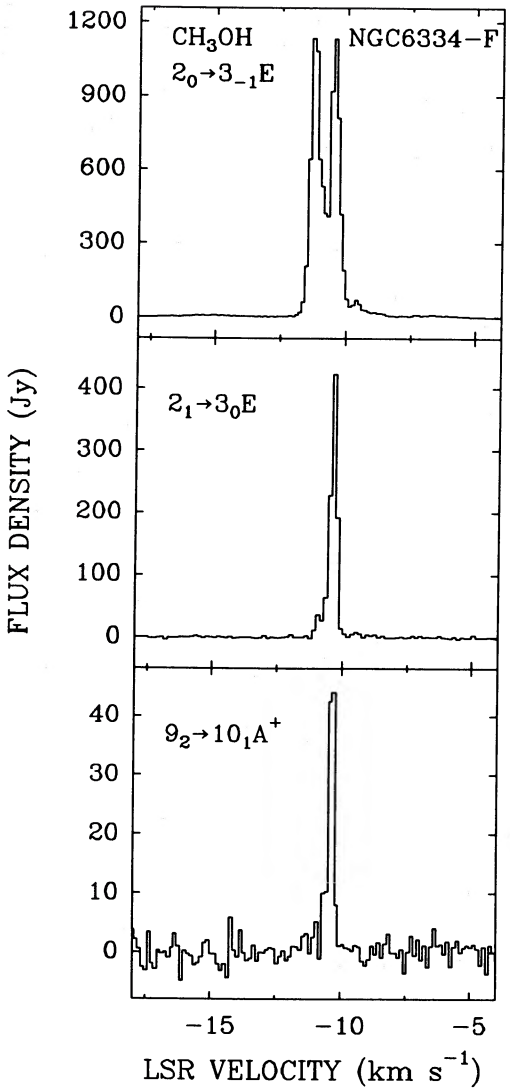

FIG. 1.—Methanol masers observed toward NGC 6334-F. *Top*: the spectrum of the 12.1 GHz $2_0 \rightarrow 3_{-1}E$ transition as observed by Batrla *et al.* (1987). *Middle and bottom panels*: our spectra of the $2_1 \rightarrow 3_0 E$ and $9_2 \rightarrow 10_1 A^+$ line at 19.9 and 23.1 GHz, respectively. Velocity resolutions are 0.12, 0.14, and 0.13 km s^{-1} for the 12.1, 19.9, and 23.1 GHz spectra, respectively.

MHz, and the other two with 2.5 MHz, so that each line could be observed at two different velocity resolutions, typically 0.25 and 0.12 km s^{-1} per channel. In the case of 25 GHz $J_2 \rightarrow J_1 E$ transitions, the $J = 2$, 3, 4, and 5 lines were observed simultaneously with the same receiver, the $J = 2$, 3, and 4 in one autocorrelator module with 10 MHz bandwidth, and the $J = 5$ line in another one with 5 MHz bandwidth. System temperatures varied between 63 and 120 K depending on frequency and weather conditions. Calibration was obtained by inserting a pulsed noise signal for half the duty cycle. This signal was measured relative to a hot-cold standard. The observing mode was position switching. Because of the source's low declination (−36°), the antenna efficiency was only ~13%. The beam size varied with frequency between 1.′7 at 19.9 GHz and 1.′2 at 25 GHz. The pointing accuracy is estimated to be better than 20″, and the absolute calibration should be good to 25%. Intensities are given as main-beam brightness temperature T_{MB} in kelvins or (for the maser lines) flux density S in janskys. At 23 GHz, 1 K T_{MB} corresponds to 3.5 Jy.

III. RESULTS

Figure 1 shows spectra of the $9_2 \rightarrow 10_1 A^+$ and $2_1 \rightarrow 3_0 E$ lines measured towards our nominal NGC 6334-F position ($\alpha_{1950} = 17^h17^m32^s.3$, $\delta_{1950} = -35°44'04''$) together with the strong $2_0 \rightarrow 3_{-1}E$ maser emission observed by Batrla *et al.* (1987). The line profiles observed in the $9_2 \rightarrow 10_1 A^+$ and $2_1 \rightarrow 3_0 E$ transitions are dominated by a single narrow spike feature. In both lines the LSR velocity of this spike (≈ −10.5 km s^{-1}) is similar to one of the most intense $2_0 \rightarrow 3_{-1}E$ emission features. In the $2_1 \rightarrow 3_0 E$ spectrum at least two other features are clearly discernible. Toward the same position, we have observed emission in the series of $J_2 \rightarrow J_1 E$ transitions ($J = 2$, 3, 4, 5, 6, 7). These lines (Fig. 2) are much broader ($v_{LSR} \approx 6$ km s^{-1}) and appear at higher velocities between −7 and −6.5 km s^{-1}. We also detect a weak broad feature at the frequency of the torsionally excited ($v_t = 1$) $10_1 \rightarrow 11_2 A^+$ transition. We searched for, but did not detect, emission from three other *A*-type methanol lines. Details of all the lines observed and derived line parameters are given in Table 1.

We also detected broad emission (Fig. 3, and Table 2), as well as two narrow emission features (Fig. 4) in the $J_2 \rightarrow J_1 E$ lines at a position 100″ north of NGC 6334-F. The northern methanol emission appears at higher velocities than the emission observed toward NGC 6334-F. The stronger one of the narrow features appears at an LSR velocity of −2.89 km s^{-1} and is detected in the $J = 4$, 5, 6, and 7 lines, while the weaker feature ($v_{LSR} = -5.24$ km s^{-1}) is only observed in the $J = 5$ and 6 lines.

In the $5_2 \rightarrow 5_1 E$ and $6_2 \rightarrow 6_1 E$ lines we made measurements at different offsets around the (0, 100″N) position, separated by 75″ (approximately one beam width). The weaker one of the narrow features and the broad emission were not detected toward these offsets. For the stronger narrow feature we determine an offset of (40″E, 110″N) relative to the F-position. The errors in this position are dominated by pointing uncertainties and should be less than 30″. Subsequently we will refer to this position as NGC 6334-I(North), the designation of a (sub)millimeter continuum source found in this direction (see § IV*b*).

IV. DISCUSSION

a) Comparison of the W3(OH) *and NGC 6334-F Methanol Masers*

The high intensities and narrow line widths observed in the $2_1 \rightarrow 3_0 E$ and $9_2 \rightarrow 10_1 A^+$ transitions strongly suggest that these lines represent high gain masers which may amplify background continuum emission from the compact NGC 6334-F radio source (Rodríguez, Cantó, and Moran 1982; Gaume and Mutel 1987). Since we have no offset measurements available, we cannot put constraints on the extent of the observed methanol emission. Thus the only *direct* evidence for maser action arises from the fact that the brightness temperature of the −10.38 km s^{-1} feature of the $2_1 \rightarrow 3_0 E$ line is 118 K, much higher than the value of 45 K one would derive for the kinetic temperature interpreting the line width of this feature as thermal broadening. It is interesting to compare the three NGC 6334-F methanol masers with their counterparts observed toward W3(OH) (Wilson *et al.* 1984; 1985; Batrla *et al.* 1987; compare Fig. 1 of Batrla *et al.* with our Fig. 1). In both

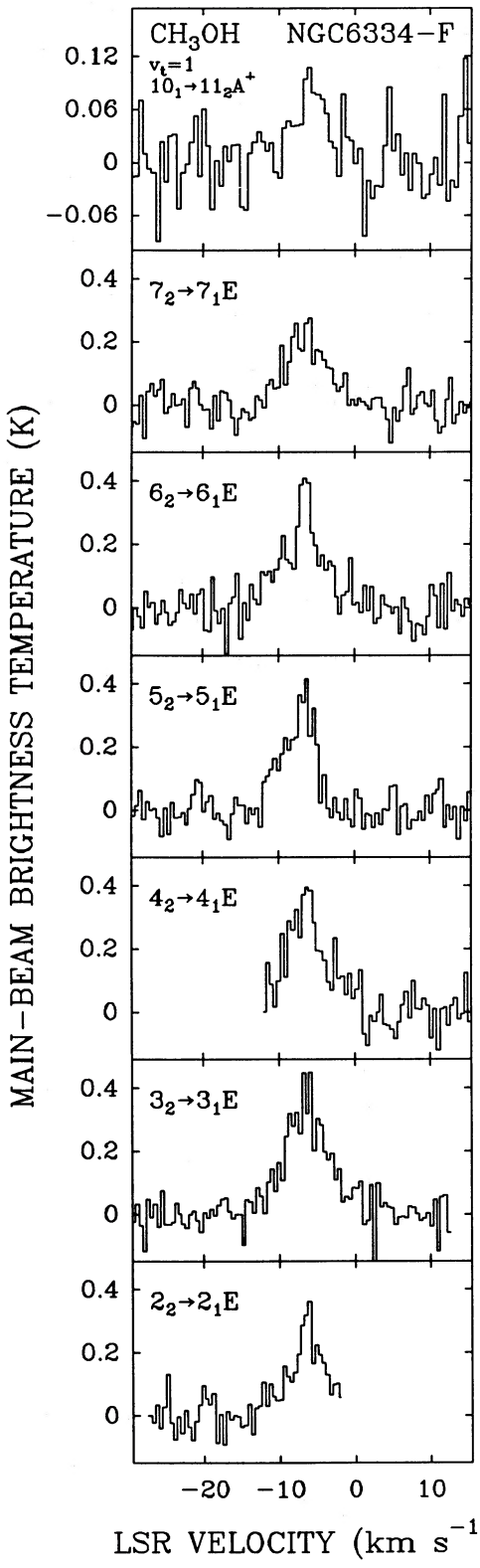

FIG. 2.—Spectra of the CH_3OH $J_{k=2} \rightarrow J_{k=1}E$ transitions and the torsionally ($v_t = 1$) excited $10_1 \rightarrow 11_2A^+$ line toward our NGC 6334-F position. Velocity resolutions are 0.56 km s^{-1} for the $10_1 \rightarrow 11_2A^+$ spectrum and 0.47 km s^{-1} for the $J_2 \rightarrow J_1E$ spectra.

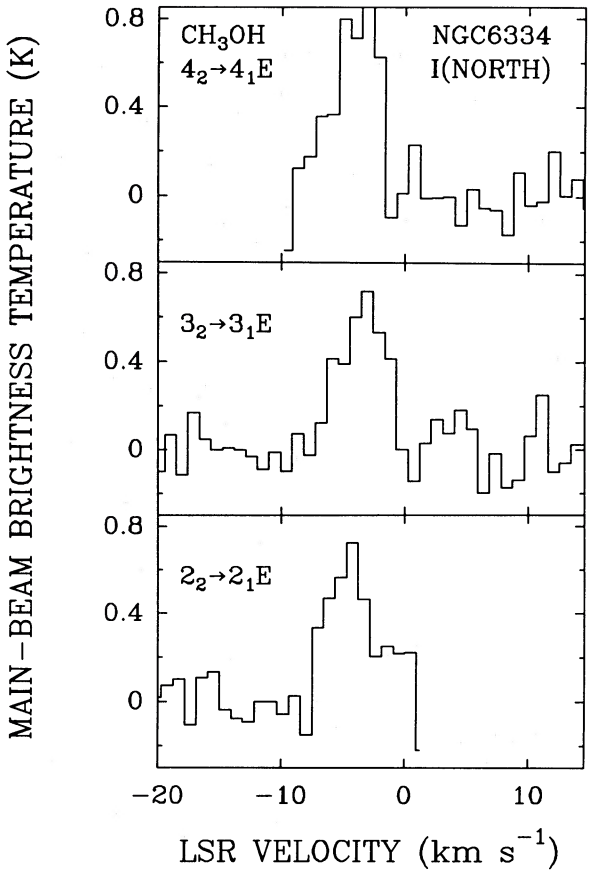

FIG. 3.—Spectra of the CH_3OH $J_{k=2} \rightarrow J_{k=1}E$ transitions ($J = 2$, 3, and 4) observed toward a position 100″ north of NGC 6334-F. In the spectra of the $4_2 \rightarrow 4_1E$ line, the intense narrow spike component (see Fig. 4) representing maser emission is clipped. The spectra have been smoothed to a velocity resolution of 0.94 km s^{-1}.

cases the $9_2 \rightarrow 10_1A^+$ line has a lower intensity than the $2_1 \rightarrow 3_0E$ which itself is weaker than the $2_0 \rightarrow 3_{-1}E$ transition. The intrinsic photon luminosities in the $9_2 \rightarrow 10_1A^+$ line are very similar in both sources and an order of magnitude lower than the values for the $2_1 \rightarrow 3_0E$ line (Table 3). It should be noted that our spectra have much lower signal-to-noise ratio than those presented by Wilson *et al.* (1984, 1985) for W3(OH) and that a number of weaker features may be hidden in the noise.

Although W3(OH) and NGC 6334-F look very similar with regard to their methanol maser emission, there is, on first look, a marked difference with regard to the broad nonmaser 25 GHz $J_2 \rightarrow J_1E$ lines. Menten *et al.* (1986*a*) have observed these transitions in *absorption* towards W3(OH), while we observe *emission* toward NGC 6334-F. It seems unlikely that the absence of absorption is due to a lack of molecular material between the H II region and the observer, because numerous OH maser condensations are clearly seen in projection against the western edge of the continuum emission (Gaume and Mutel 1987). By analogy with W3(OH), one would expect the methanol masers to be coexistent with the OH. This is also indicated by the fact that the OH (allowing for Zeeman splitting) and methanol masers cover the same velocity range (-10 to -11 km s^{-1}). In contrast, the nonmaser CH_3OH emission observed in the 25 GHz lines is centered at ≈ -6.5 km s^{-1}.

TABLE 1

K-BAND CH_3OH LINES OBSERVED TOWARD NGC 6334-F

v_t	Transition	Frequency[a] (MHz)	E_l[b] (cm^{-1})	Intensity[c] (Jy or K)	v_{LSR} (km s^{-1})	Δv (km s^{-1})	Notes
			$^{12}CH_3OH$ Maser Lines				
0.....	$2_1 \rightarrow 3_0 E$	19967.3961(2)[d]	13.3	37.4(1.7) Jy	−10.76(0.03)	0.56(0.07)	e,f
				412.7(5.7)	−10.38(0.01)	0.28(0.01)	...
				6.4(1.2)	−9.47(0.06)	0.64(0.14)	...
0.....	$9_2 \rightarrow 10_1 A^+$	23121.0242(5)[d]	98.1	51.6(2.0)	−10.36(0.01)	0.25(0.01)	g
			$^{12}CH_3OH$ Nonmaser lines				
0.....	$2_2 \rightarrow 2_1 E$	24934.382(5)[h]	14.0	0.26(0.03) K	−6.28(0.22)	5.70(0.66)	i
0.....	$3_2 \rightarrow 3_1 E$	24928.70(10)	18.8	0.36(0.03)	−6.46(0.18)	6.87(0.47)	i
0.....	$4_2 \rightarrow 4_1 E$	24933.468(2)[h]	25.3	0.32(0.04)	−6.68(0.27)	7.08(0.80)	i
0.....	$5_2 \rightarrow 5_1 E$	24959.080(2)[h]	33.3	0.34(0.03)	−7.16(0.19)	4.96(0.43)	j
0.....	$6_2 \rightarrow 6_1 E$	25018.123(2)[h]	43.0	0.29(0.04)	−6.77(0.29)	6.17(0.84)	j
0.....	$7_2 \rightarrow 7_1 E$	25124.873(2)[h]	54.3	0.23(0.03)	−6.47(0.30)	6.27(0.68)	j
0.....	$10_1 \rightarrow 9_2 A^-$	23444.82(10)	98.8	<1.1	...	...	
0.....	$11_1 \rightarrow 10_2 A^+$	20171.07(10)	115.0	<0.84	...	...	
1.....	$10_1 \rightarrow 11_2 A^+$	20970.65(5)	313.7	0.10(0.03)	−5.73(0.59)	4.81(1.75)	k
1.....	$12_2 \rightarrow 11_1 A^-$	21550.31(5)	332.2	<0.75	...	...	...
			$^{13}CH_3OH$				
0.....	$2_0 \rightarrow 3_{-1} E$	14782.15(10)[l]	8.0	<0.39 Jy	...	...	...

NOTES.—Errors are 1 σ deviations determined by Gaussian fits.

[a] Frequencies are taken from Lovas 1984 unless otherwise noted.

[b] Excitation energy of lower level relative to the $1_{-1} E$ and $0_0 A$ levels for E- and A-type transitions, respectively.

[c] For maser lines, intensities are given as peak flux densities (in Jy units). Nonmaser line intensities are given in Kelvin peak main-beam brightness temperature. When no line was detected, 3 σ upper limits are given.

[d] Frequency taken from Mehrotra, Dreizler, and Mäder 1985.

[e] Three independent Gaussians fitted.

[f] Velocity resolution 0.15 km s^{-1}.

[g] Velocity resolution 0.13 km s^{-1}.

[h] Frequencies taken from Gaines, Casleton, and Kukolich 1974.

[i] Velocity resolution 0.47 km s^{-1}.

[j] Velocity resolution 0.23 km s^{-1}.

[k] Velocity resolution 0.28 km s^{-1}.

[l] Frequency taken from Anderson, Herbst, and De Lucia 1987.

Jackson, Ho, and Haschick (1988) have mapped the emission from the (1, 1) line of ammonia (NH_3) toward NGC 6334-F using the VLA. They find the emission to emerge from two separate regions, one to the west and the other to the northeast of the compact continuum source. They interpret this morphology together with the fact that both regions have differing velocities as the signature of a rotating toroidal structure. As in the case of the nonmaser methanol, no ammonia is observed in absorption.

TABLE 2

THERMAL CH_3OH $J_2 \rightarrow J_1 E$ EMISSION OBSERVED TOWARD NGC 6334-I (NORTH)

Transition	T_{MB}[a] (K)	v_{LSR} (km s^{-1})	Δv (km s^{-1})	Notes
$2_2 \rightarrow 2_1 E$.....	0.66(0.16)	−4.6(0.3)	4.0(0.8)	b
$3_2 \rightarrow 3_1 E$.....	0.71(0.18)	−3.3(0.4)	3.9(0.6)	b
$4_2 \rightarrow 4_1 E$.....	0.73(0.19)	−4.9(0.3)	3.7(0.8)	b,c
$5_2 \rightarrow 5_1 E$.....	<0.9	...	...	c
$6_2 \rightarrow 6_1 E$.....	<0.7	...	...	c
$7_2 \rightarrow 7_1 E$.....	<1.0	...	...	c

NOTES.—Errors are 1 σ deviations determined by Gaussian fits.

[a] Peak main-beam brightness temperature. When no line was detected, 3 σ upper limits are given.

[b] Velocity resolution 0.47 km s^{-1}.

[c] Narrow maser emission detected. See text for discussion.

In summary, the bulk of the molecular material probed by the ammonia and, most likely, the broad $J_{k=2} \rightarrow J_{k=1} E$ methanol emission is found offset from the H II region, while the OH and, by inference, the methanol masers appear to be located in a narrow interface region between the western ammonia clump and the H II region, part of which is seen in projection against the continuum emission. We note that toward W3(OH) the $9_2 \rightarrow 10_1 A^+$ methanol masers are also found in a narrow strip that delineates the edge of a more extended region containing molecular gas (Menten *et al.* 1988*b*).

TABLE 3

NGC 6334-F AND W3(OH) CLASS B METHANOL MASERS

Transition	Isotropic Photon Luminosity[a] (Photons s^{-1})		Notes
	NGC 6334-F	W3(OH)	
$9_2 \rightarrow 10_1 A^+$	2.4×10^{43}	2.2×10^{43}	b
$2_1 \rightarrow 3_0 E$	2.6×10^{44}	2.5×10^{44}	c
$2_0 \rightarrow 3_{-1} E$	2.0×10^{45}	3.8×10^{45}	d

[a] Distances of 1.7 and 2.2 kpc were assumed for NGC 6334-F and W3(OH), respectively.

[b] W3(OH) value calculated from Wilson *et al.* 1984.

[c] W3(OH) value calculated from Wilson *et al.* 1985.

[d] Values from Batrla *et al.* 1987.

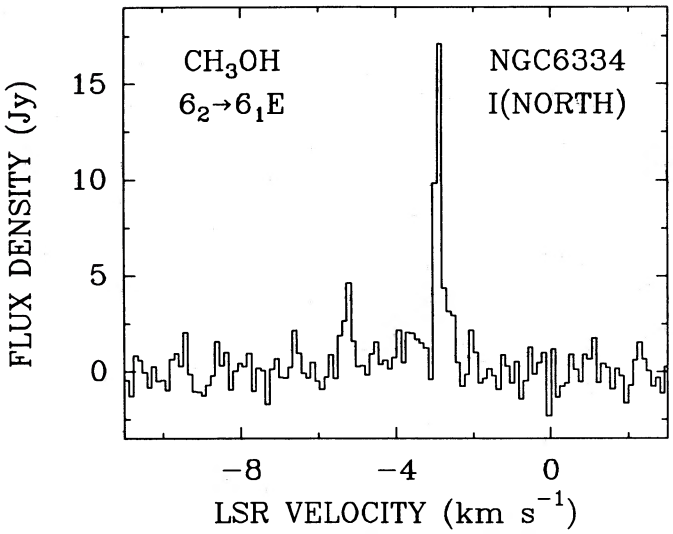

FIG. 4.—Spectrum of the CH_3OH $6_2 \rightarrow 6_1E$ transition taken toward a position 100″ north of NGC 6334-F. The velocity resolution is 0.12 km s^{-1}.

b) Properties of the Thermal Emission

The broad thermal emission observed in the 25 GHz lines covers a velocity range that includes the whole range of NH_3 velocities observed by Jackson, Ho, and Haschick (1988). Nevertheless, it is not obvious that the methanol and ammonia distributions are identical. Experience with other regions, in particular Orion-KL (Menten *et al.* 1988*c*), shows that this is not necessarily the case. Clearly, high-resolution (VLA) observations are needed to allow a detailed analysis. To determine the properties of the methanol emission averaged over our 75″ beam, we have used the rotation temperature diagram method (see, e.g., Johansson *et al.* 1984). Figure 5 shows that the values calculated from the $J_2 \rightarrow J_1E$ lines can be well fitted by a straight line, yielding a rotation temperature T_{rot} of 36 ± 3 K and a total methanol column density $N(CH_3OH)$ of $3.1 \pm 0.4 \times 10^{15}$ cm^{-2}. The torsionally excited $10_1 \rightarrow 11_2 A^+$ line at an excitation of 451 K has been excluded from the fit because its intensity is anomalously high (see § IV*e*).

The thermal emission from the $J_2 \rightarrow J_1E$ lines observed toward NGC 6334-I(North), 100″ north of NGC 6334-F,

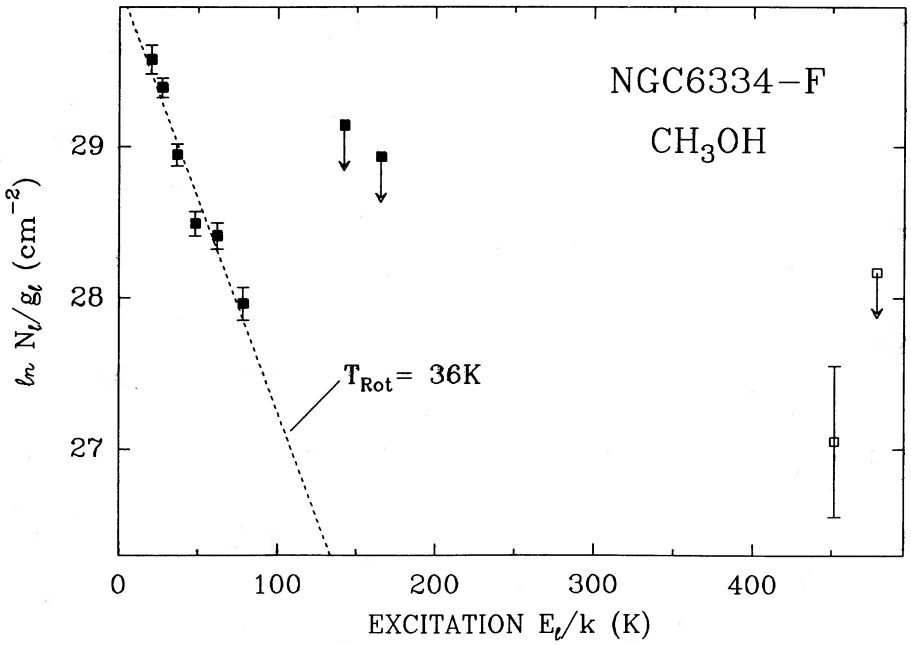

FIG. 5.—Rotation temperature diagram for a number of K band methanol transitions observed toward NGC 6334-F. Filled symbols mark transitions from the torsional ground state, open symbols denote transitions within the first torsionally excited ($v_t = 1$) state. The dotted line represents a fit to the $J_2 \rightarrow J_1E$ lines only, which are represented by the six leftmost points. The rotation temperature and CH_3OH column density resulting from the fit are 36 K and 3.1×10^{15} cm^{-2}, respectively.

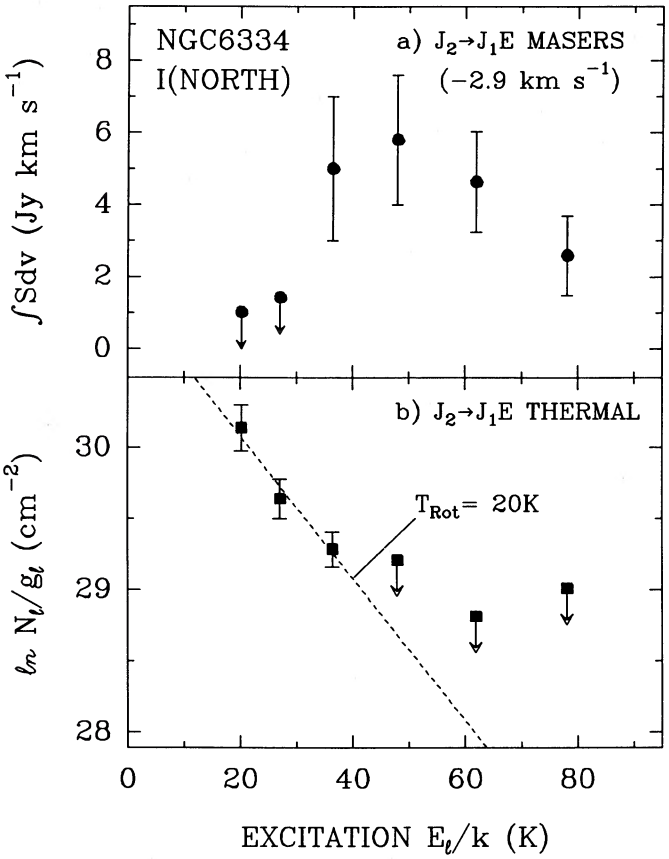

FIG. 6.—(*a*) Integrated flux densities of the $J_2 \rightarrow J_1E$ masers (J = 2, 3, 4, 5, 6, and 7) observed toward NGC 6334-I(North) are plotted against the excitation energies of the lines. The error bars correspond to 30% uncertainties which are caused by pointing and calibration errors. (*b*) Rotation temperature diagram for the broad thermal emission from the CH_3OH $J_2 \rightarrow J_1E$ transitions observed toward NGC 6334-I(North). The dotted line represents a fit to the J = 2, 3, and 4 transitions which are represented by the three leftmost points. The rotation temperature and CH_3OH column density resulting from the fit are 20 K and 3.6 × 10^{15} cm^{-2}, respectively.

appears at higher velocities (−4 km s^{-1}) and has a narrower line width (3.8 km s^{-1}) than its southern counterpart. The rotation diagram method (Fig. 6*b*) yields $T_{rot} = 20 \pm 6$ K and $N(CH_3OH) = 3.6 \pm 1.5 \times 10^{15}$ cm^{-2}. These parameters are less well determined than in the case of NGC 6334-F, due to the poorer signal-to-noise ratio for our data taken toward the northern position.

It is interesting to compare the properties of the methanol emission with FIR observations, especially since the FIR beam sizes usually employed are similar to our resolution. Loughran *et al.* (1986) report multiband observations centered at wavelengths of 21, 42, 71, and 134 μm. Source I (the FIR source associated with the H II region NGC 6334-F) is detected in all bands and is coincident with a 71 μm optical depth peak and a dust temperature (T_D) peak. T_D, the 71–134 μm color temperature, peaks at a value of 40 K which is very similar to the CH_3OH rotation temperature derived by us. In the higher frequency (21 and 42 μm) bands, no emission is observed north of source I. At lower frequencies another source appears ∼2′ to the north of NGC 6334-I. At 400 μm, I(North) is equal in intensity to source I (Gezari 1982), and at 1 mm the northern source dominates (Cheung *et al.* 1978). Gezari derives T_D values of 33 and 19 K, and H_2 column densities of 2 × 10^{23} and 1 × 10^{24} cm^{-2} for I and I(North), respectively. Assuming, like Gezari, a source size of 1′, we derive an abundance ratio of $[CH_3OH/H_2] = 4 \times 10^{-8}$ for the southern and 1 × 10^{-8} for the northern methanol emission. This is somewhat lower than the $[CH_3OH/H_2]$ values of 10^{-7}–10^{-6} found in other warm molecular cloud cores (Menten *et al.* 1986*a*). One should, however, keep in mind the uncertainties in the determination of the H_2 column density and the unknown actual extent of the CH_3OH emission.

c) $J_2 \rightarrow J_1E$ Masers toward NGC 6334-I(North)

The narrow emission features in the $J_2 \rightarrow J_1E$ transitions are coincident, within the positional errors, with the northern (sub)millimeter continuum source. Because of the extremely narrow line widths (Δv = 0.22 km s^{-1}), we assume that they represent maser emission. In Figure 6*a* we plot the integrated flux densities of the −2.89 km s^{-1} maser component measured in the different lines of the $J_2 \rightarrow J_1E$ series versus the excitation energy of the lines. The strongest emission is observed in the J = 5 or 6 line. This is also observed in the case of 25 GHz masers associated with other regions (Menten *et al.* 1986*a*).

d) Class A and Class B Methanol Masers in the NGC 6334 Region

The properties of the $J_2 \rightarrow J_1E$ masers 2′ north of NGC 6334-F closely resemble the properties of masers detected in these lines toward other molecular clouds (Menten *et al.* 1986*a*): (*a*) The spectra show only a few features; (*b*) single features emerge from different spots separated typically by tens of arcseconds; (*c*) the maser positions are offset, in some cases by several parsecs, from compact H II regions and prominent OH maser centers. These masers, designated *class A* methanol masers by Batrla *et al.* (1987), have very different properties from the *class B* masers observed in the 12.1, 19.9, and 23.1 GHz lines. The latter methanol masers are most frequently observed in the 12.1 GHz $2_0 \rightarrow 3_{-1}E$ transition. W3(OH) and NGC 6334-F are the only known sources which are also masing in the 19.9 and 23.1 GHz lines. Class B masers usually show many spectral features which cover the same velocity range as the OH emission observed in the same sources. The association with OH, as well as the fact that the emission regions appear to be projected on compact continuum emission, has been directly established by interferometric observations in the cases of W3(OH), NGC 7538, and Cepheus A (Menten *et al.* 1988*a*, *b*). NGC 6334-F and NGC 6334-I(North) exemplify the different nature of class B and class A methanol maser regions, respectively (Fig. 7). The class B masers are found in a more evolved region where an H II region has already formed, whereas no H II is observed toward the northern methanol emission region containing the class A masers. One might speculate that class A methanol masers probe the earliest phases in the formation of massive stars.

e) The Anomalously Strong Torsionally Excited $10_1 \rightarrow 11_2 A^+$ Line

Inspection of our rotation temperature diagram (Fig. 5) immediately shows that the intensity of the torsionally excited v_t = 1, $10_1 \rightarrow 11_2 A^+$ transition observed toward NGC 6334-F is much too high to be consistent with the straight line which represents an excellent fit to the ground-state $J_2 \rightarrow J_1E$ data. Using the rotation temperature and methanol column density derived from the fit to the $J_2 \rightarrow J_1E$ data, one predicts an

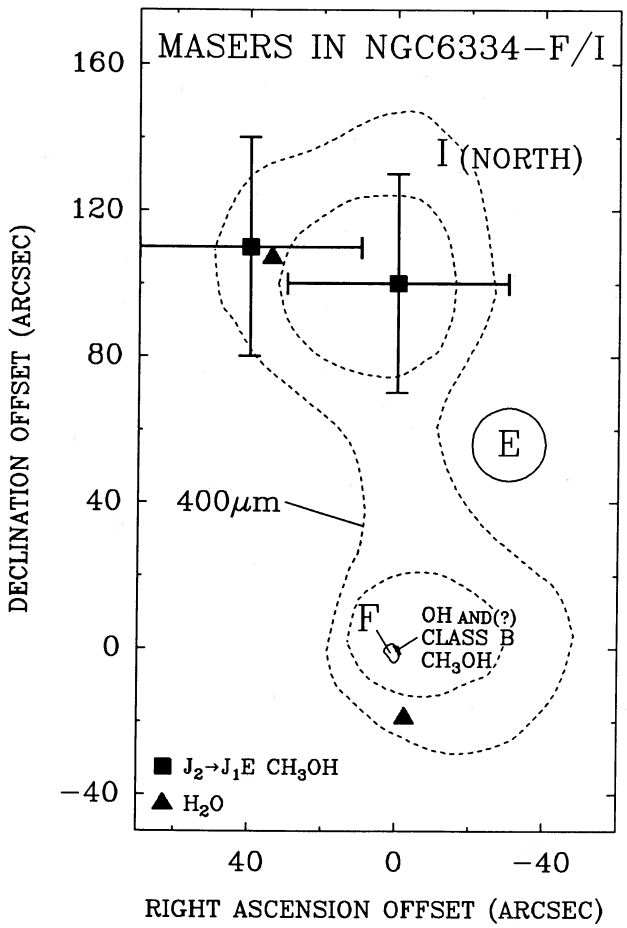

FIG. 7.—The distribution of different molecular maser species in the NGC 6334-F/I(North) region. The (0, 0) position corresponds to (α_{1950} = 17^{h}17^{m}32^s.3, δ_{1950} = −35°44′04″). The squares denote the positions of the 25 GHz methanol masers. The triangles mark the water masers detected by Moran and Rodríguez (1980). The H_2O positions have approximately the same uncertainties (30″) as our 25 GHz positions. The OH masers (Gaume and Mutel 1987; Zheng *et al.* 1988) lie on the western edge of the compact H II region F which is indicated by the 10% contour of the 15 GHz continuum map of Gaume and Mutel (1987). Class B methanol masers as observed in the 12.1, 19.9, and 23.1 GHz lines are most likely to be coexistent with the OH masers. The circle gives the approximate size of the extended radio source E of Rodríguez, Cantó, and Moran (1982), and the dotted contours represent 50% and 80% of the peak 400 μm flux density as measured by Gezari (1982).

intensity of 6×10^{-6} K for the $v_t = 1$, $10_1 \rightarrow 11_2 A^+$ line which is more than four orders of magnitude lower than the observed value of 0.1 K. This result strongly suggests that there exists a hot component in the methanol emission core associated with NGC 6334-F. Menten *et al.* (1986*b*) found a similar discrepancy for the $10_1 \rightarrow 11_2 A^+$ line observed toward W3(OH).

Excitation of CH_3OH molecules to the first torsionally excited ($v_t = 1$) state is subject to the selection rule $\Delta k = \pm 1$, but not 0. Therefore, if the $k = 2$ ladder of A-type methanol in the torsional ground state ($v_t = 0$) is overpopulated relative to the $k = 1$ ladder, then in the $v_t = 1$ state the opposite is true (Menten *et al.* 1986*b*). In both W3(OH) and NGC 6334-F, the existence of the 23.1 GHz $9_2 \rightarrow 10_1 A^+$ maser, as well as the recently detected masers in the 38 GHz $6_2 \rightarrow 5_3 A^+$ and A^- transitions (Haschick, Baan, and Menten 1989), suggest that the $k = 2$ ladder is overpopulated relative to its neighboring ladders. On the other hand, one would expect that rotational transitions inside the $v_t = 1$ state which have their upper level in the $k = 1$ and lower level in the $k = 2$ ladder might be inverted. One such transition is the torsionally excited $10_1 \rightarrow 11_2 A^+$ line, and it is possible that the observed anomalously high intensity of this line is due to maser action. One difficulty with this scheme is that, in the case of NGC 6334-F, the velocity of the $10_1 \rightarrow 11_2 A^+$ line is definitely higher than the velocity of the $9_2 \rightarrow 10_1 A^+$ maser.

f) Nondetection of the $^{13}CH_3OH$ $2_0 \rightarrow 3_{-1}E$ Line

We have searched for, but not detected, the $^{13}CH_3OH$ isotopic counterpart of the $2_0 \rightarrow 3_{-1}E$ transition. Apart from the fact that the frequencies of $^{13}CH_3OH$ transitions are slightly different from those of the $^{12}CH_3OH$ main isotope, the energy level structures of both isotopic species are equivalent. Comparing our 3 σ upper limit (Table 1) with the measured intensity of the $^{12}CH_3OH$ maser (Batrla *et al.* 1987; see also Fig. 1), we calculate that for the strongest features, the emission in the $2_0 \rightarrow 3_{-1}E$ line of the main isotope is at least 2000 times more intense than its $^{13}CH_3OH$ equivalent. Because collisional pumps as well as pump mechanisms involving (far-)infrared continuum radiation work equally well for both isotopes, one might expect maser emission in the $2_0 \rightarrow 3_{-1}E$ line also from ^{13}C methanol. Our upper limit puts some, although not very tight, constraints on the properties of such a possible $^{13}CH_3OH$ maser.

Since the output of a collisionally pumped and saturated maser is proportional to the density of the maser molecules (e.g. Elitzur 1982), maser emission from the $^{13}CH_3OH$ $2_0 \rightarrow 3_{-1}E$ line should have been easily detectable, if a normal isotopic abundance ratio ($[^{12}C/^{13}C] = 89$) is assumed. It is, of course, possible that the lower density of $^{13}CH_3OH$ molecules is not sufficient to saturate the maser, while the $^{12}CH_3OH$ emission is saturated. The output of a radiatively pumped and saturated maser is proportional to the pump rate and does not depend on the density. In this case, a $^{13}CH_3OH$ maser would be equally strong as a $^{12}CH_3OH$ maser (if the $^{13}CH_3OH$ density was high enough to cause saturation) but undetectably weak otherwise.

V. SUMMARY

We have observed a number of CH_3OH lines in the 19–25 GHz range toward the H II region NGC 6334-F and toward a cool (sub)millimeter continuum source, NGC 6334-I(North), to the north of the H II region. Toward NGC 633-F, we detect maser emission in the $2_1 \rightarrow 3_0 E$ and $9_2 \rightarrow 10_1 A^+$ GHz transitions. The only other known region showing maser emission in these lines is W3(OH), and it seems that both regions are very similar with respect to their methanol and OH masers. We detect broad thermal emission in the $J_2 \rightarrow J_1$ lines of *E*-type methanol toward NGC 6334-F and toward NGC 6334-I(North). The rotational temperatures are similar to the dust temperatures derived for these regions. However, the detection of a line from the first torsionally excited state of methanol points to the existence of a very hot emission component associated with the H II region.

Toward the northern source we also detect maser emission in the $J_2 \rightarrow J_1 E$ lines but do not detect masers in the $2_1 \rightarrow 3_0 E$, $9_2 \rightarrow 10_1 A^+$, or the 12.1 GHz $2_0 \rightarrow 3_{-1}E$ transitions which are associated with H II regions and OH masers. $J_2 \rightarrow J_1 E$ masers seem to arise toward less evolved, maybe protostellar, regions with no detectable centimeter continuum emission.

We searched for but did not detect the $^{13}CH_3OH$ isotopic counterpart of the $2_0 \rightarrow 3_{-1}E$ maser transition. We conclude that a possible $^{13}CH_3OH$ $2_0 \rightarrow 3_{-1}E$ maser is not saturated.

We would like to thank J. M. Moran, M. J. Reid, C. M. Walmsley, and an anonymous referee for their comments on the manuscipt.

REFERENCES

Anderson, T., Herbst, E., and De Lucia, F. C. 1987, *Ap. J. Suppl.*, **64**, 703.
Barrett, A. H., Schwartz, P. R., and Waters, J. W. 1971, *Ap. J. (Letters)*, **168**, L101.
Batrla, W., Matthews, H. E., Menten, K. M., and Walmsley, C. M. 1987, *Nature*, **326**, 49.
Cheung, L. H., Frogel, J. A., Gezari, D. Y., and Hauser, M. G. 1978, *Ap. J. (Letters)*, **226**, L149.
Elitzur, M. 1982, *Rev. Mod. Phys.*, **54**, 1225.
Gaines, L., Casleton, K. H., and Kukolich, S. G. 1974, *Ap. J. (Letters)*, **191**, L99.
Gaume, R. A., and Mutel, R. L. 1987, *Ap. J. Suppl.*, **65**, 193.
Gezari, D. Y. 1982, *Ap. J. (Letters)*, **259**, L29.
Haschick, A. H., Baan, W. A., and Menten, K. M. 1989, *Ap. J.*, submitted.
Jackson, J. M., Ho, P. T. P., and Haschick, A. D. 1988, *Ap. J. (Letters)*, **333**, L73.
Johansson, L. E. B., *et al.* 1984, *Astr. Ap.*, **130**, 227.
Koo, B.-C., Williams, D. R. W., Heiles, C., and Backer, D. C. 1988, *Ap. J.*, **326**, 931.
Loughran, L., McBreen, B., Fazio, G. G., Rengarajan, T. N., Maxson, C. W., Serio, S., Sciortino, S., and Ray, T. P. 1986, *Ap. J.*, **303**, 629.
Lovas, F. J. 1984, SLAIM Magnetic Tape Version I-84, private communication.
Mehrotra, S. C., Dreizler, H., and Mäder, H. 1985, *Zs. Naturforsch.*, **40a**, 683.
Menten, K. M., Johnston, K. J., Wadiak, E. J., Walmsley, C. M., and Wilson, T. L. 1988*a*, *Ap. J. (Letters)*, **331**, L41.
Menten, K. M., Reid, M. J., Moran, J. M., Wilson, T. L., Johnston, K. J., and Batrla, W. 1988*b*, *Ap. J. (Letters)*, **333**, L83.
Menten, K. M., Walmsley, C. M., Henkel, C., and Wilson, T. L. 1986*a*, *Astr. Ap.*, **157**, 318.
———. 1988*c*, *Astr. Ap.*, **198**, 253.
Menten, K. M., Walmsley, C. M., Henkel, C., Wilson, T. L., Snyder, L. E., Hollis, J. M., and Lovas, F. J. 1986*b*, *Astr. Ap.*, **169**, 271.
Moran, J. M., and Rodríguez, L. F. 1980, *Ap. J. (Letters)*, **236**, L159.
Norris, R. P., Caswell, J. L., Gardner, F. F., and Wellington, K. J. 1987, *Ap. J. (Letters)*, **321**, L159.
Rodríguez, L. F., Cantó, J., and Moran, J. M. 1982, *Ap. J.*, **255**, 103.
Wilson, T. L., Walmsley, C. M., Menten, K. M., and Hermsen, W. 1985, *Astr. Ap.*, **147**, L19.
Wilson, T. L., Walmsley, C. M., Snyder, L. E., and Jewell, P. R. 1984, *Astr. Ap.*, **134**, L7.
Zheng, X. W., Moran, J. M., Reid, M. J., Schneps, M. H., Garcia-Barreto, J. A., and Garay, G. 1988, in *The Impact of VLBI on Astrophysics and Geophysics*, ed. M. J. Reid and J. M. Moran (Dordrecht: Kluwer), p. 263.

WOLFGANG BATRLA: NRAO, P.O. Box 2, Green Bank, WV 24922

KARL M. MENTEN: Harvard-Smithsonian Center for Astrophysics, 60 Garden Street, Cambridge, MA 02138